

Minor Galaxy Interactions: Star Formation Rates and Galaxy Properties

Deborah Freedman Woods

*Department of Astronomy, Harvard University
60 Garden St., Cambridge, MA 02138*

dwoods@cfa.harvard.edu

Margaret J. Geller

*Smithsonian Astrophysical Observatory
60 Garden St., Cambridge, MA 02138*

ABSTRACT

We study star formation in a sample of 1204 galaxies in minor ($|\Delta m_z| \geq 2$) pairs and compact groups, drawn from the Sloan Digital Sky Survey Data Release 5 (SDSS DR5). We analyze an analogous sample of 2409 galaxies in major ($|\Delta m_z| < 2$) pairs and compact groups to ensure that our selection reproduces previous results, and we use a “field” sample of 65,570 galaxies for comparison. Our major and minor pairs samples include only galaxies in spectroscopically confirmed pairs, where the recessional velocity separation $\Delta V < 500 \text{ km s}^{-1}$ and the projected spatial separation $\Delta D < 50 \text{ kpc h}^{-1}$. The relative magnitude (a proxy for the mass ratio) of the pair is an important parameter in the effectiveness of the tidally triggered star formation in minor interactions. As expected, the secondary galaxies in minor pairs show evidence for tidally triggered star formation, whereas the primary galaxies in the minor pairs do not. The galaxy color is also an important parameter in the effectiveness of triggered star formation in the major galaxy pairs. In the major pairs sample, there is a correlation between the specific H α star formation rate (SSFR) and ΔD in the blue primary and blue secondary galaxies; for the red primary and red secondary galaxies, there is none. Galaxies in pairs have a higher mean SSFR at every absolute magnitude compared to matched sets of field galaxies, and the relative increase in mean SSFR becomes larger with decreasing intrinsic luminosity. We also detect a significantly increased AGN fraction in the pair galaxies compared to matched sets of field galaxies.

Subject headings: galaxies: evolution – galaxies: interactions – galaxies: stellar content

1. Introduction

Observations of apparently interacting galaxies in nearby systems reveal enhanced star formation compared to non-interacting galaxies. Larson & Tinsley (1978) first showed that systems

in the Atlas of Peculiar Galaxies (Arp 1966) have a wider range of optical colors and star formation rates than typical galaxies. Observations of increased star formation activity in galaxy interactions include measurements of H α and other optical emission lines (Kennicutt & Keel 1984; Kennicutt et al. 1987; Keel 1993; Liu & Kennicutt 1995a; Donzelli & Pastoriza 1997; Barton et al. 2000, 2003; Lambas et al. 2003; Nikolic et al. 2004; Kauffmann et al. 2004), infrared emission (Kennicutt et al. 1987; Jones & Stein 1989; Sekiguchi & Wolstencroft 1992; Keel 1993; Nikolic et al. 2004; Geller et al. 2006), radio continuum emission (Hummel 1981), and galaxy colors (Larson & Tinsley 1978; Geller et al. 2006). Struck (2005) reviews galaxy collisions.

Numerical simulations of major galaxy interactions account for the general features of the observations. The simulations of Toomre & Toomre (1972) first demonstrated that gravitational interactions between galaxies produce disrupted morphologies like those observed. Other early simulations describe how galaxy mergers deposit gas in the centers of merger remnants (Negroponte & White 1983; Hernquist 1989; Barnes & Hernquist 1991). Central star formation in interacting galaxies results from gaseous inflows that occur when the gas loses angular momentum through gravitational tidal torques produced primarily by the non-axisymmetric structure induced by the companion galaxy (Mihos & Hernquist 1996). The galaxy structure strongly influences the strength and timing of the burst of star formation triggered by the gaseous inflows (e.g. Mihos & Hernquist 1996; Tissera et al. 2002). The simulations of Cox et al. (2006) model colliding disk galaxies with feedback from massive stars and radiative cooling, and use a density-dependent star formation prescription; they produce a centrally concentrated burst of star formation for simulations with a range of star formation histories. (See the introduction in Cox et al. (2006) for a concise summary of galaxy merger simulations.)

Simulations of the Milky Way Galaxy and Large Magellanic Cloud (LMC) interaction suggest that there should be an asymmetry in the response to the gravitational interaction of the primary and secondary galaxies in minor interactions¹. Mastropietro et al. (2005) show in their simulations of the Milky Way Galaxy and LMC interaction that the LMC experiences tidal disruption causing an elongated disc, bar creation, warped profile, diffuse stellar halo, and gas loss from the LMC’s disc. Meanwhile, the Milky Way disc shows essentially no response to the encounter. The simulations of Mayer et al. (2001) of the Milky Way and dwarf irregular galaxies reveal central infall of gas and gas stripping in the dwarf irregular galaxies. The high central surface brightness dwarf galaxies experience a single, strong burst of central star formation; the low central surface brightness dwarf galaxies experience multiple smaller epochs of star formation. There is, however, a plausible mechanism for induced star formation in the major galaxies: simulations show that tidal torques from minor companions provoke non-axisymmetric structure in the main disk galaxy, causing the gas to lose its angular momentum and fall inward, presumably leading to central star formation (Hernquist & Mihos 1995).

¹To avoid potentially confusing language, we refer to galaxy pairs with magnitude difference $|\Delta m| < 2$ as “major” pairs, and those with $|\Delta m| \geq 2$ as “minor” pairs. In both cases, we refer to the more luminous galaxy in the pair as

There is debate over the connection between galaxy interactions and enhanced AGN activity. A number of studies investigate the enhanced AGN fraction in interacting systems (Dahari 1985; Keel 1985; Bushouse 1987; Kelm et al. 2004; Alonso et al. 2007) and the possible excess of companions to Seyfert galaxies (Fuentes-Williams et al. 1988; Schmitt 2001). Although the results have not always agreed, there is growing observational evidence for interaction-driven nuclear activity (e.g. Hennawi et al. 2006; Serber et al. 2006).

Large data sets enable statistical analysis of the relationship between star formation and pair properties. In their sample of ~ 500 galaxies drawn from the CfA2 Redshift Survey, Barton et al. (2000) show that the equivalent width of the $\text{H}\alpha$ emission ($\text{EW}(\text{H}\alpha)$) is anti-correlated with the projected galaxy pair separation (ΔD). Numerous additional studies confirm the anti-correlation between star formation indicators and projected separation in the SDSS (Nikolic et al. 2004), the 2dF Survey (Lambas et al. 2003), and the CfA2 Redshift Survey plus infrared data (Geller et al. 2006). The galaxy pairs identified in these data sets are dominated by major interactions, where the magnitude differences in the systems are small. This property of pair samples is a natural consequence of the magnitude distribution in magnitude-limited redshift surveys; pairs with large magnitude difference reside in the tails of the distribution. Targeted searches for high contrast pairs have inherently low success rates because the background galaxies outnumber the probable companions.

Although difficult to identify, minor companions are particularly interesting because they play a critical role in the formation and evolution of galaxies (Somerville & Primack 1999; Kauffmann et al. 1999a,b; Diaferio et al. 1999). Hierarchical structure formation models show that galaxies grow by accreting other galaxies, most often minor companions (see the merger tree in Wechsler et al. 2002). Minor mergers may be at least an order of magnitude more common than major mergers over the course of history (see Hernquist & Mihos (1995) and references therein). Despite their role in galaxy formation models, observational studies of minor interactions are rare. A study of minor interactions from the CfA2 Redshift Survey and follow-up observations by Woods et al. (2006) includes 57 galaxies with magnitude difference ($|\Delta m_r| > 2$). Woods et al. find that star formation activity in their sample of minor interactions is not enhanced as strongly as it is in major interactions; however, their small data set precludes analyzing the primary and secondary galaxies separately.

Here we address the effectiveness of minor interactions in triggering star formation. We examine the way the effectiveness differs in the primary and secondary galaxies. We also study how intrinsic galaxy properties including luminosity and color influence the triggered star formation in both major and minor interactions. We also investigate the preferential association of AGNs with interacting systems. We assume the standard flat ΛCDM cosmological model with a Hubble constant of $H_0 = 71 \text{ km s}^{-1} \text{ Mpc}^{-1}$ and $\Omega_m h^2 = 0.135$ (Spergel et al. 2003), and we use the convention $H_0 = 100h$.

the “primary” galaxy, and the less luminous as the “secondary” galaxy.

In §2, we discuss the selection of the major and minor pairs samples, and of the field galaxy sample used for comparison. We describe the samples’ properties in §3, including absolute and relative magnitudes, and colors. We discuss the relative abundance of AGN in various samples and their relation to pair properties in §4. The star formation rates in our pairs samples and field sample are discussed in §5. We compare the star formation rates with pair properties in §6 and with galaxy properties in §7. We conclude in §8.

2. Sample Selection

2.1. Galaxy Pairs Selection

Although minor interactions must occur frequently in the galaxy formation process (e.g. Wechsler et al. 2002), they are not well observed. Identifying minor companions observationally is challenging because magnitude limited redshift surveys naturally contain relatively more pairs of similar magnitude, and because directed searches for low-luminosity companions around primary galaxies have inherently low success rates due to contamination by the more abundant background galaxies (Woods et al. 2006). The frequency of false pairs, especially for the case of minor companions, makes it essential to have spectroscopic confirmation of coincidence in redshift space.

The sheer size of the Sloan Digital Sky Survey Data Release 5 (SDSS DR5) with more than 8,000 square degrees of the sky observed and spectra for 674,749 galaxies to $m_r = 17.77$ allows us to find a significant sample of high contrast pairs¹. York et al. (2000) contains a technical summary of SDSS; Gunn et al. (1998) describe the camera; Gunn et al. (2006) describe the telescope; Fukugita et al. (1996) has the sdss filter definitions; Strauss et al. (2002) introduces the Main Galaxy Sample; and Adelman-McCarthy et al. (2006) contains a description of DR4 (no DR5 summary paper exists to date).

We select our pair sample with projected physical separation $\Delta D < 50 \text{ kpc h}^{-1}$ and line-of-sight velocity separation $\Delta V < 500 \text{ km s}^{-1}$ from the nearest neighbor. To minimize aperture effects, we restrict our sample to the redshift range $8,000 < cz < 50,000 \text{ km s}^{-1}$, and we require that at least 20% of the total galaxy luminosity lands in the fiber. Kewley et al. (2005) demonstrate that a covering fraction of > 20% is necessary to avoid substantial differences in nuclear and global measurements of star formation rates, extinction, and metallicity in their sample of 101 galaxies from the Nearby Field Galaxy Survey (Jansen et al. 2000a,b). The main effect of this criterion is to exclude very extended nearby galaxies. Although this selection introduces a slight bias toward centrally concentrated galaxies at low redshift, that bias is the same for the pair and field galaxy samples.

We further refine our sample to avoid rich clusters and to reduce the influence from other

¹Sloan Digital Sky Survey. 2007, SDSS Website: <http://www.sdss.org/dr5/>

neighboring galaxies. To minimize effects of the morphology-density relation (Dressler 1980) or the SFR-density relation (Gómez et al. 2003; Lewis et al. 2002; Hashimoto et al. 1998), we exclude galaxies within $\Delta D < 1.5 \text{ Mpc h}^{-1}$ (~ 1 virial radius) and $\Delta V < 5000 \text{ km s}^{-1}$ of rich Abell clusters. Rines et al. (2005) show in their Cluster and Infall Region Nearby Survey (CAIRNS) that outside 2-3 virial radii from the cluster center, the fraction of galaxies with H α star formation detected in their inner disks is comparable to that of the field. Moreover, the distribution of star formation rates is independent of global density (Rines et al. 2005; Carter et al. 2001). In the context of galaxy interactions, the gravitational tidal interaction can potentially trigger enhanced star formation activity whenever the galaxy contains enough gas. Galaxies not in clusters are more likely to have substantial gas available for star formation, providing a stronger signal of the interaction.

After constructing the initial pairs catalog, we further exclude galaxies that have another apparent photometric companion ($|\Delta m_z| < 2$, compared to the primary) without a measured redshift and located at smaller projected separation than the spectroscopically confirmed companion. Otherwise, in our measurements of ΔD and $|\Delta m_z|$, it would be unclear which galaxy is actually the nearest projected neighbor. Because we compare each galaxy to its nearest neighbor, there are situations where we include only partial pairs in the final analysis. Only one member of an apparent group may meet our requirement that no closest companion lacks spectroscopy; other members of the group may fail the test. We also accept partial pairs in the case where one member of the pair fails to meet our aperture test or has a poor quality spectrum, but has a reliable magnitude and redshift reported allowing measurement of ΔD and $|\Delta m_z|$.

The spectroscopic data for our sample, including the spectral line fits, come from the Princeton reductions of the SDSS DR5. The photometric data are provided by the SDSS DR5. We take our data from local copies of the SDSS and Princeton datasets, maintained at the Harvard-Smithsonian Center for Astrophysics. We select the sample in SDSS Petrosian z -band for the best correspondence between luminosity and mass, and we divide it into subsets of major and minor interactions.

Nikolic et al. (2004) show that SDSS z -band Petrosian magnitudes provide an unbiased estimator of galaxy mass in SDSS pairs by comparing the m_z with total K -band magnitudes from the Two-Micron All-Sky Survey (2MASS) Extended Source Catalog (XSC; Jarret et al. 2000), which are nearly independent of extinction. The primary galaxies in our sample have $m_z < 17.77$, which is a subset of the galaxies within the SDSS spectroscopy completeness limit of $m_r < 17.77$, but provides consistency when using z -band photometry. All of the magnitudes quoted in this paper are Petrosian (Petrosian 1976; Strauss et al. 2002).

We use the H α emission line to calculate the star formation rate of our pair and field galaxies. We require that H α and H β flux have signal-to-noise ratio > 3 for accurate measurement of specific H α star formation rates (SSFRs) using optical data. Numerous studies demonstrate an anti-correlation between star formation indicators and projected separation, using a variety of star formation indicators. Barton et al. (2000, 2003) and Woods et al. (2006) use EW(H α). The EW

measurement is independent of reddening, unlike the $\text{H}\alpha$ star formation rate. A complete census of interacting galaxies, including highly reddened objects, requires infrared data (Geller et al. 2006). The galaxy pairs in Geller et al. show an anti-correlation between star formation rate and ΔD , for both far-IR and $\text{EW}(\text{H}\alpha)$ star formation indicators, as do the galaxy pairs in Nikolic et al. (2004).

Visual inspection of all of the pair galaxies allows us to eliminate some false pairs from our sample. The main problem we find is the automated deblending of a single extended galaxy into multiple galaxies, each with different photometric and spectroscopic measurements. We estimate that $\sim 15\%$ of the minor pairs with projected separation $\Delta D < 50 \text{ kpc h}^{-1}$ are actually a poorly deblended galaxy. This problem is most common for potential pairs at small projected separation. We choose not to exclude all galaxies that are flagged by SDSS as deblended because doing so would eliminate substantial numbers of real pairs at small projected separation, which are important for our sample. Failure to inspect the close pairs, however, could be problematic for galaxy counts and other measurements.

Although this paper focuses on the star formation properties of the minor galaxy pairs, we include the major galaxy pairs to make sure that our selection reproduces previous results. Major galaxy pairs have been well studied, but the difference in sample selection can make it difficult to draw direct comparisons between minor and major pairs samples. By constructing a sample of major companions with exactly the same selection effects as the minor companions, we can draw a better comparison between the two sets of pairs.

The sample of minor mergers, defined here as $|\Delta m_z| \geq 2$, comprises 1204 galaxies in pairs or compact groups. The sample of major mergers, defined here as $|\Delta m_z| < 2$, has 2409 galaxies in pairs and compact groups. A magnitude difference $|\Delta m_z| = 2$ corresponds to a mass ratio of ~ 6 , assuming a constant mass-to-light ratio across the M_z range.

We note that both the major and minor pairs samples are deficient in pairs with small projected separations (Figure 1). The true distribution should be nearly flat across ΔD because the slope of the two-point galaxy-galaxy correlation function is ~ -2 at small separation (Padmanabhan et al. 2006). For the ΔD distribution of a more complete sample of galaxy pairs, see Geller et al. (2006).

SDSS fiber constraints result in pairs samples that are deficient in small projected separations. This bias is particularly unfortunate for studying tidally triggered star formation because the strongest bursts of star formation are, of course, expected in pairs with small ΔD (e.g. Barton et al. 2000). The results derived from the sample lacking small ΔD pairs are not as strong as would be expected in a sample with a flat distribution: there are relatively fewer galaxies with the possibility for showing the strongest bursts of star formation, and there is a greater probability for outliers at large ΔD where the sample is larger. Re-sampling the distribution to flatten it would in principle provide a better representation of SSFR at different ΔD , but the reduction in sample size would also weaken the statistical significance of the results. We analyze the SDSS sample without attempting to correct for incompleteness and take detections of trends as strong indicators of the underlying tidal triggering.

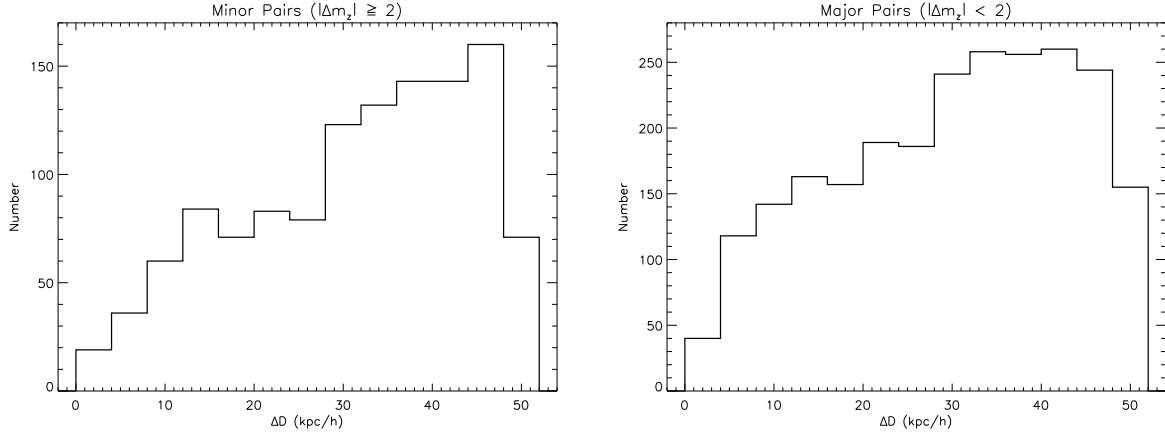


Fig. 1.— The distribution of projected separations ΔD for the minor pairs (above left) and major pairs (above right). Both pairs samples are deficient in pairs with small ΔD : the distribution for a complete sample is expected to be flat across all ΔD .

2.2. Field Galaxy Sample Selection

For comparison, we select a field galaxy sample with the same criteria for the pairs sample. The galaxies lie in the redshift range $8,000 < cz < 50,000 \text{ km s}^{-1}$ and have at least 20% of the total galaxy luminosity in the fiber. We limit the sample to $b > 40^\circ$ to keep the sample size manageable. We exclude galaxies from dense regions ($\Delta D < 1.5 \text{ Mpc h}^{-1}$ and $\Delta V < 5000 \text{ km s}^{-1}$ of rich Abell clusters) from the field sample. There are 65,570 galaxies that meet our selection criteria. The field galaxy sample properties are discussed in §3.

3. Sample Properties

The galaxies we select are at low redshift (Figure 2). The minor pairs are concentrated in the lowest redshift bins because they must be close enough that the faint companion galaxy is brighter than the SDSS spectroscopic magnitude limit, $m_r = 17.77$.

Our sample of major interactions includes pairs with $|\Delta m_z| < 2$, and is weighted toward pairs with $|\Delta m_z| \sim 2$. This distribution is consistent with a greater fractional abundance of relatively low luminosity galaxies. The minor pairs sample includes galaxies within $2 < |\Delta m_z| < 6$, and has more galaxies with smaller magnitude differences. The median $|\Delta m_z|$ for the major and minor pairs is 1.5 magnitudes, and the median $|\Delta m_z|$ of the minor pairs is 2.6. The galaxies with greater $|\Delta m_z|$ are relatively rare because the available volume for these pairs is small in a magnitude limited sample.

Figure 3 shows the distribution of magnitude differences for both the major and minor pairs samples. The absolute magnitude distribution of minor pair galaxies is clearly bimodal; the distri-

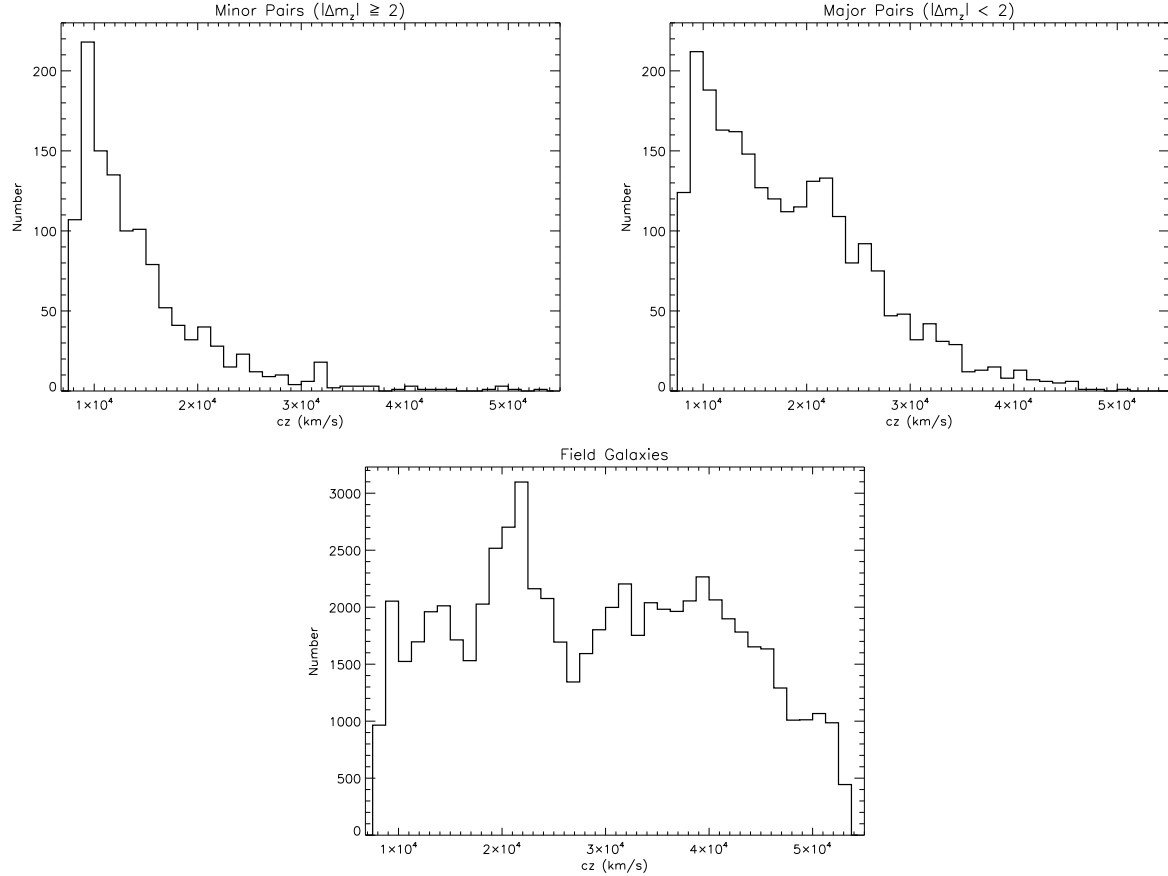


Fig. 2.— The distribution of recessional velocities for the minor pairs (top left), major pairs (top right), and field sample (bottom center). The minor pairs must be at lower cz in order for the secondary galaxy to be observable.

bution of M_z of the primary galaxy has a median of -22.4, and the distribution for the secondary galaxies has a median of -19.6 (see Figure 4.) Almost all (97%) of the primary galaxies are brighter than $M_z^* \simeq -20.7$, and most (80%) of the secondaries are fainter [M_z^* estimated from $M_r^* = -20.49$; Ball et al. (2006)]. The major pairs sample shows more similar distributions of M_z for the primary and secondary galaxy, although it is still bimodal. The median M_z of the primary galaxies is -22.1, and the median of the secondary galaxies is -21.0.

We classify our galaxies as red or blue based on the $u - r$ color and the absolute magnitude M_r , as prescribed in Baldry et al. (2004). Because lower luminosity galaxies tend to be bluer, the fraction of blue galaxies is related to the mean sample magnitude: in our minor pairs sample, 18% (111/608) of the primary galaxies are blue, and 40% (238/596) of the secondary galaxies are blue. In the major pairs, 24% (292/1195) of the primary galaxies are blue and 32% (390/1214) of the secondary galaxies are blue. Figure 5 shows the color-magnitude diagrams for the minor and major

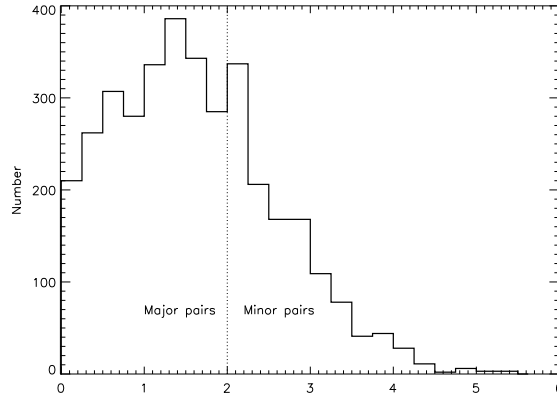


Fig. 3.— The distribution of apparent magnitude differences. This plot shows both the major ($|\Delta m_z| < 2$) and the minor ($|\Delta m_z| \geq 2$) galaxy pairs. The median $|\Delta m_z|$ for the combined major and minor pairs is 1.5.

pairs samples; Figure 6 shows the same diagrams for the field galaxies’.

Galaxies in our pairs samples with different absolute magnitude distributions should have intrinsic differences in star formation rates, colors, and AGN fractions. Our goal is to distinguish the intrinsic differences from those attributed to the gravitational tidal interaction.

Galaxy colors are well correlated with gas content, star formation rates, and other galaxy properties (e.g. Sandage & Visvanathan 1976; Baldry et al. 2004; Bernardi et al. 2003; Conselice 2006). Figure 5 shows that the secondary galaxies tend to be bluer than the primary galaxies. Because blue galaxies generally have a greater gas content, they are more likely to show enhanced central star formation as a result of a gravitational tidal interaction. The simulations of Barnes & Hernquist (1996) demonstrate the importance of gas content for tidally triggered star formation. However, blue galaxies are also more likely to have intrinsically high specific star formation rates, independent of the interaction. Thus we look for two measures of the interaction: (1) enhanced SSFR in pairs overall compared to field galaxies, and (2) enhanced SSFR as a function of ΔD , which can be attributed to tidal triggering.

4. Galaxy Classification: Relative Abundances of Starforming Galaxies, Composites, or AGNs

We use emission line ratios to classify galaxies as starforming galaxies, composites, or AGNs (Figures 7,8, and 9), according to the definitions in Kewley et al. (2006). Separating the starforming galaxies from the AGNs is necessary for a clean measurement of galaxy star formation rates. Our SSFR indicator is a function of the H α emission, and thus we select for galaxies in which starforming

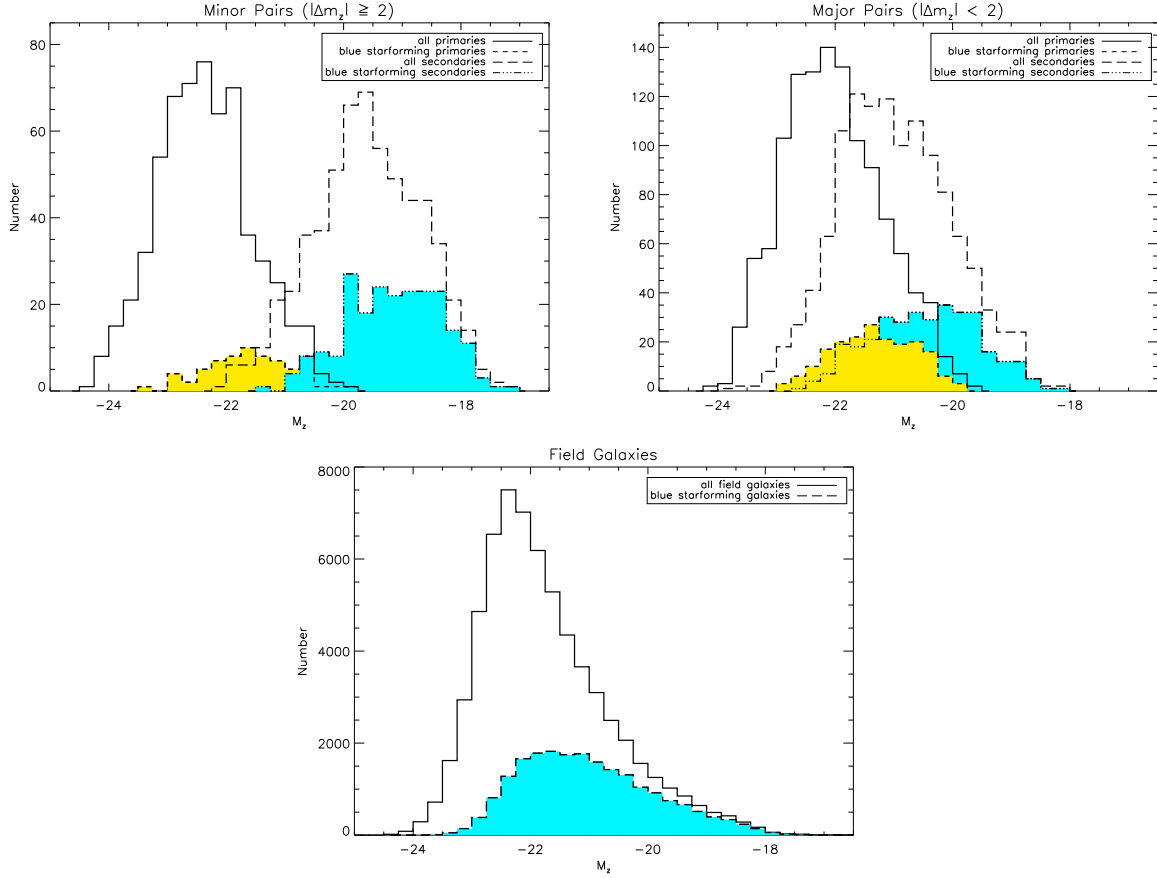


Fig. 4.— Distribution of M_z for the minor pairs (top left), major pairs (top right), and field galaxies (bottom center).

regions, not AGN, dominate the H α emission. We maximize our sample size of starforming galaxies by accepting cases that potentially harbor a weak AGN, where the dominant contribution to the H α emission probably originates from starforming regions. To that end, we require a signal-to-noise ratio > 3 in H α and H β to ensure an accurate reddening correction to the H α star formation rate. We do not impose limits on the signal-to-noise in [O III] and [N II] because weak [O III] and [N II] emission lines indicate weak or no AGN activity. The scatter in small [O III]/H β and small [N II]/H α is due to noisy values of small [O III] and [N II].

Our aperture requirement of at least 20% of the galaxy light landing in the fiber introduces a slight bias toward centrally concentrated galaxies. Centrally concentrated galaxies are more likely to be early-type (Strateva et al. 2001), and to harbor an AGN (Alonso et al. 2007). However, because the spectra include a significant fraction of the galaxy light, it is harder to observe weak AGNs against the background galaxy. Because we cannot eliminate these selection effects, we control for them by maintaining the same selection criteria for the minor pairs, major pairs, and

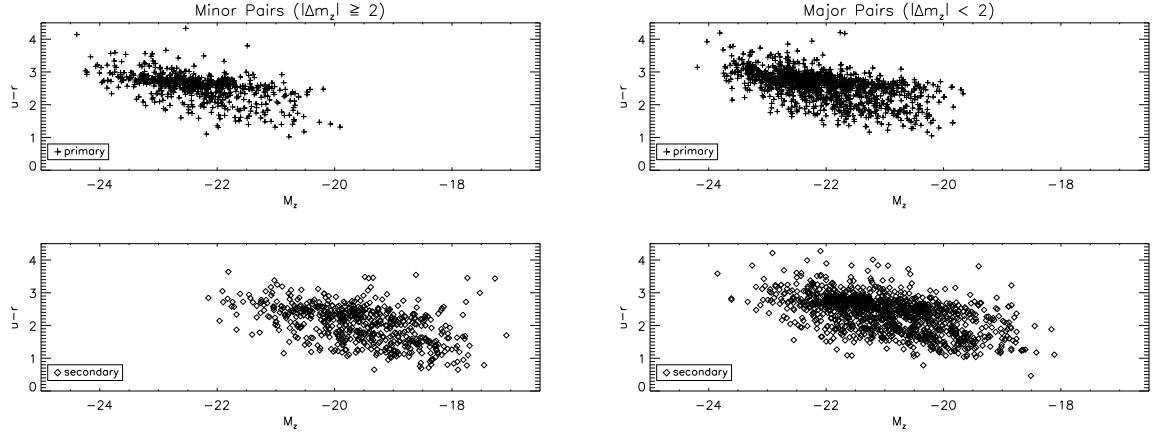


Fig. 5.— The $u - r$ color-magnitude diagram for the galaxies in minor pairs (above left) and in major pairs (above right).

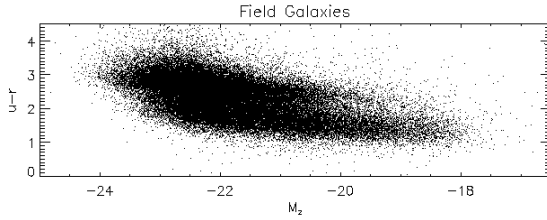


Fig. 6.— The bimodal color distribution can be seen in the field galaxy sample, which spans a wide range of M_z .

field samples.

The different pairs samples show very different AGN fractions, ranging from 2.1% in the minor secondary galaxies to 29% in the minor primary galaxies. The field galaxies are 8% AGNs. The subsets containing the more luminous galaxies have a larger AGN fraction; the median M_z of all primary galaxies in the minor pairs sample is -22.4 , compared to a median of $M_z = -19.6$ for all secondary galaxies in the minor pairs sample (Figure 4). Our AGN fractions for the various pairs samples are consistent with the observed trend of increasing AGN fraction with increasing galaxy luminosity (Kauffmann et al. 2003b; Best et al. 2005).

We compare the AGN fraction of the galaxies in our pairs samples with matched subsets of galaxies from our field sample. We select a subset of field galaxies having the same distribution of M_z and the same number of red and blue galaxies as in the corresponding pairs sample. Repeating the random selection for 5,000 trials, we find the average percentages of starforming galaxies, composites, and AGNs in our representative sets of field galaxies. Table 1 shows the classification for the pairs samples and for the matched sets of field galaxies.

The primary galaxies in both the major pairs and the minor pairs show statistically significant

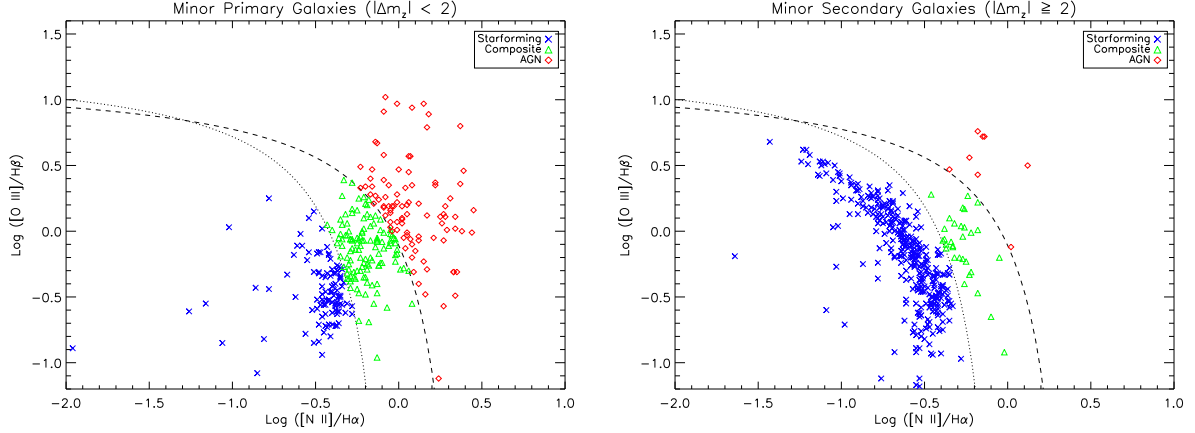


Fig. 7.— Classification of the primary galaxies (above left) and secondary galaxies (above right) in minor pairs as starforming, composite, or AGN using the Kewley et al. (2006) prescriptions. The samples with greater intrinsic luminosities have larger AGN fractions (Table 1).

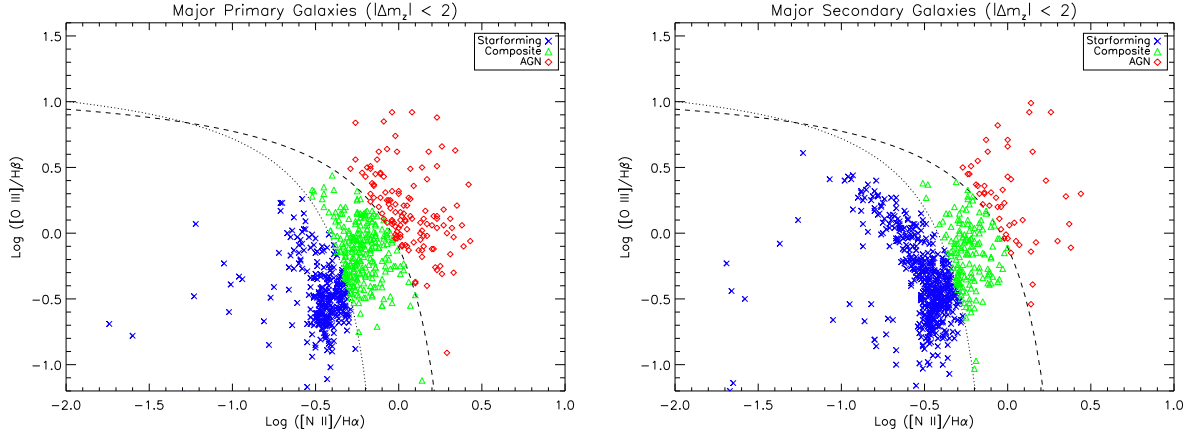


Fig. 8.— Classification of the primary galaxies (above left) and secondary galaxies (above right) in major pairs as starforming, composite, or AGN using the Kewley et al. (2006) prescriptions. The samples with greater intrinsic luminosities have larger AGN fractions (Table 1).

increases in AGN fraction (a 5σ increase for the minor primaries and a 7σ increase for the major primaries.) Because the field galaxy subsets are selected to have the same distribution of M_z and the same number of red and blue galaxies as their counterpart pairs samples, the correlation between galaxy luminosity and AGN fraction cannot explain the differences. For the primary galaxies in the minor pairs, it may be the case that more than one secondary galaxy is present. We do not have the data to count the number of minor companions. However, our selection does require that the primary galaxies have no major companions within $\Delta D = 50$ kpc h^{-1} and $\Delta V = 500$ km s^{-1} (§2). It is clear that having at least one minor companion increases the odds that a galaxy harbors

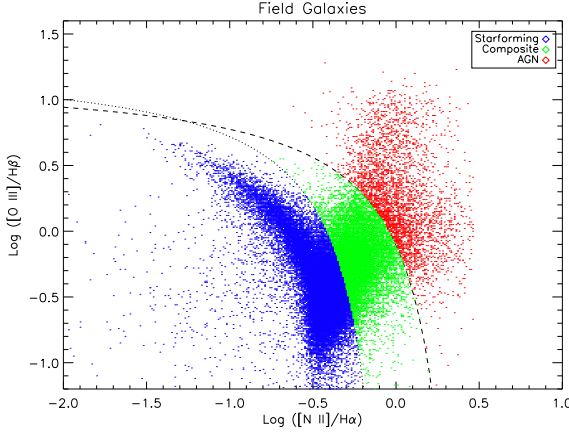


Fig. 9.— Classification of the field galaxies as starforming, composite, or AGN using the Kewley et al. (2006) prescriptions.

Table 1: Galaxy classification in minor pairs, major pairs, and field galaxies.

Sample	Sample Size	Classified ^a	Starforming	Composite	AGN	AGN in Field ^b
Minor primary	608	324	34%	38%	29%	14%
Minor secondary	596	377	90%	8.2%	2.1%	2.0%
Major primary	1195	686	45%	34%	18%	12%
Major secondary	1214	709	71%	22%	7%	6%
Total field	65,570	41,894	64%	27%	8%	...

^aClassified galaxies must have measurable emission in [N II], H α , [O III], and H β , and the H α and H β flux have signal-to-noise ratios > 3 .

^bThe matched field sample represents the average over 5,000 random draws of field galaxies with the same distribution of M_z and the same numbers of red and blue galaxies that are in the corresponding pairs sample.

an AGN.

The increased AGN fraction in our pairs samples is generally consistent with the recent work of Alonso et al. (2007), who find a 10% excess of AGN in SDSS pair galaxies compared to their reference sample. However, our different sample selection prohibits a direct comparison with their work (the Alonso et al. sample includes only pairs that exhibit signs of tidal interaction on visual inspection.) Numerous prior works have investigated the association of AGN activity and galaxy interactions (e.g. Dahari 1985; Keel 1985; Fuentes-Williams et al. 1988; Kelm et al. 2004), and there is some debate over the role of galaxy interactions in triggering AGN activity. Recent observational studies by Hennawi et al. (2006) and Serber et al. (2006) suggest that AGN activity is associated with local companions, in agreement with the numerical modeling of Kauffmann & Haehnelt (2000); Hopkins et al. (2006).

A plot of the AGN fraction as a function of ΔD also hints at enhanced AGN activity for the primary galaxies in the minor pairs (Figure 10). We detect the trend in AGN fraction versus ΔD at only the 1 to 2σ level. A larger data set of pairs at small projected separation would help to determine the relationship between AGN activity and gravitational tidal interactions. We note that the size of the spectroscopic aperture influences our ability to detect AGNs against the more luminous host galaxies; our sample is selected to have galaxies with $\geq 20\%$ of the light in the fiber. Nuclear spectra would allow for the classification of weaker AGNs. Considering our limited ability to identify AGNs, and the dearth of pairs at small ΔD , the observed correlation of AGN fraction with ΔD is potentially very interesting, but requires further investigation with a larger data set.

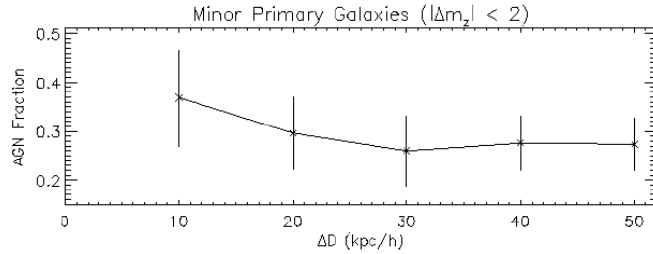


Fig. 10.— The fraction of galaxies classified as AGN according to the definitions in Kewley et al. (2006) for the primary galaxies in minor galaxy pairs.

The galaxies in major pairs do not show an obvious trend in AGN fraction versus ΔD . The effects of our aperture requirement and the absence of pairs at small ΔD may be washing out the results for the major pairs, although it is unclear why the trend for the minor primaries can be measured despite these effects. We note that a smaller percentage of galaxies in the major pairs are classified as AGN across all ΔD compared to the minor pairs (Table 1), perhaps due to their different distributions of intrinsic luminosities. A larger sample of major pairs at small ΔD would help to clarify the relationship between AGN fraction and pair properties.

5. Distribution of Specific Star Formation Rates in Pairs and Field Galaxies

After removing the AGN and composite objects from our pairs and field samples, we investigate the star formation properties for the starforming galaxies. References to SSFR in our samples from hereon refer to the starforming galaxies only, unless specified otherwise. We use the Hopkins et al. (2003) prescription for calculating the H α star formation rate based on the SDSS observed H α flux. The H α SFR of Hopkins et al. utilizes the H α luminosity ($L_{H\alpha}$) calibration from Kennicutt (1998):

$$SFR_{H\alpha}(M_{\odot} \text{ yr}^{-1}) = \frac{L_{H\alpha}}{1.27 \times 10^{34} W}. \quad (1)$$

To calculate the $L_{H\alpha}$ from the SDSS H α flux, Hopkins et al. prescribe corrections for aperture size and for obscuration by dust in the target galaxy. We use the Balmer ratio to correct for dust

obscuration and the “alternative aperture correction” term that is proportional to $r_{Petro} - r_{fiber}$ (see Equation B3 in Hopkins et al.) To derive the specific star formation rate (SSFR) from the SFR, we normalize the SFR by the M_z of the galaxy, where the normalization factor assumes $1M_\odot = 1L_\odot$ in the z -band and $M_{z(\odot)} = 4.52$ (Yasuda et al. 2001). Figure 11 shows the distribution of SSFR in the field galaxies sample.

As shown in §3, the major and minor pairs, and the primary and secondary galaxies within those pairs have different characteristic colors and absolute magnitudes. To make a fair comparison of SSFR distributions between the various pairs samples and the field sample, we select subsets of the field sample with the same distributions of absolute magnitudes and the same proportion of red and blue galaxies as the relevant pairs sample. We repeat the selection of the matched field galaxy subset for 5,000 random trials, and then measure the Kolmogorov-Smirnov (K-S) probability that the distributions of SSFR are drawn from the same parent distribution, averaged over the 5,000 random trials.

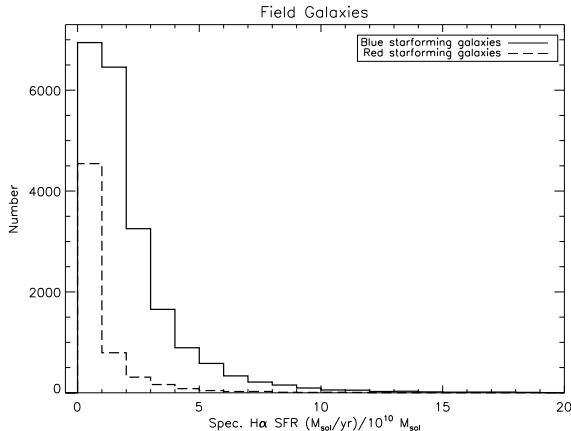


Fig. 11.— Distribution of SSFR for the entire field galaxy sample. There are a few objects with $20 < \text{SSFR} > 100$, which make up 0.20% (42/21490) of the blue starforming galaxies, and $5.5 \times 10^{-2}\%$ (3/5411) of the red starforming galaxies.

Both primary and secondary galaxies in the major pairs sample have distributions of SSFR that differ from the matched sets of field galaxies. For the blue starforming primary galaxies, the K-S probability of the SSFR deriving from the same parent sample as the matched subset of field galaxies is $P_{KS} = 5.5 \times 10^{-2}$; for the secondary blue starforming galaxies, the K-S probability is $P_{KS} = 7.0 \times 10^{-3}$. As a sanity check, we measure the K-S probability of the magnitude distributions deriving from the same parent samples, and find $P_{KS} = 0.97$ and 0.83 for the primary and secondary blue starforming galaxies, confirming that the magnitude distributions are consistent with having the same parent distribution. The blue starforming galaxies, both primary and secondary, tend to have a larger proportion of high SSFRs, compared to the field galaxies. Figures 12 and 13 show the SSFR distributions for the red and blue major pair galaxies, along with the average SSFR

distributions for the 5,000 random trials of matching field galaxy subsets.

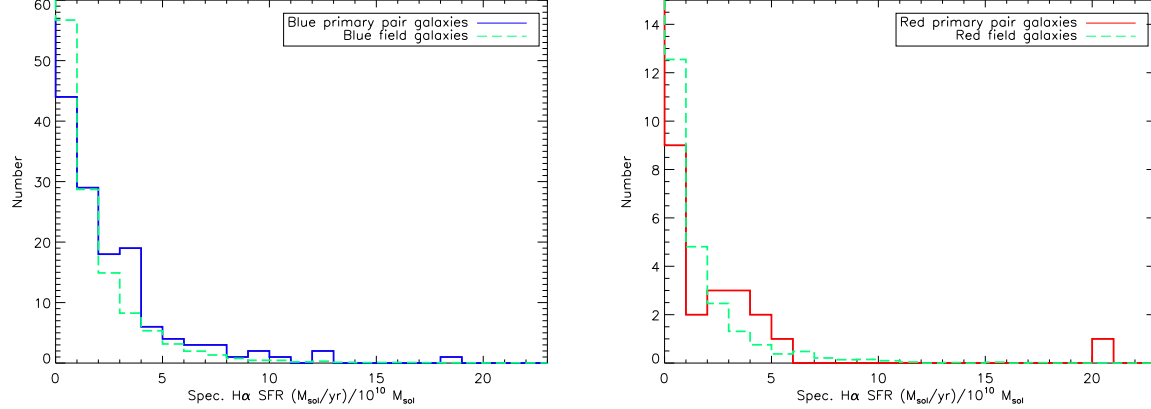


Fig. 12.— Distribution of SSFR for the primary galaxies in the major pairs sample that are blue (above left) or red (above right), along with the average distribution of SSFR for the matched sets of field galaxies.

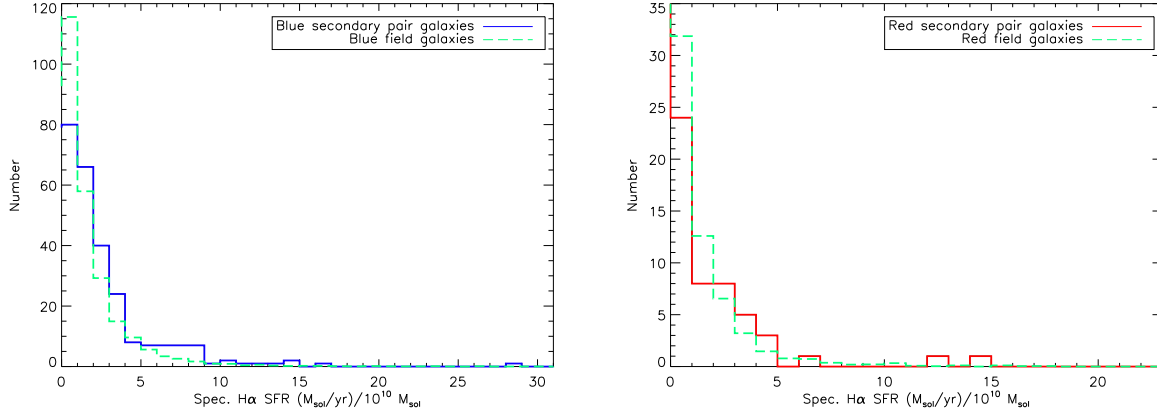


Fig. 13.— Distribution of SSFR for the blue secondary galaxies (above left) and the red secondary galaxies (above right) in the major pairs sample, along with the average distribution of SSFR for the matched sets of field galaxies.

For the minor pairs sample, we find that the distributions of the SSFR of the primary or secondary blue starforming galaxies do not differ significantly from those of the matched subsets of field galaxies. Figures 5 and 5 show the SSFR distributions of the red and blue minor pair galaxies, and the average SSFR distributions of the random selection of field galaxies with matched absolute magnitude and color distributions. A larger sample of pairs at small ΔD might yield a difference in the SSFR distributions because that is where the strongest signal is expected. A problematic aspect of testing the minor pairs against a field sample is that minor companions should be very

common. It is possible that many of our low luminosity field galaxies are also associated with minor interactions. In contrast, major interactions are less common, which may explain why we measure differences in the SSFR distributions for the major pairs and matched field galaxy samples.

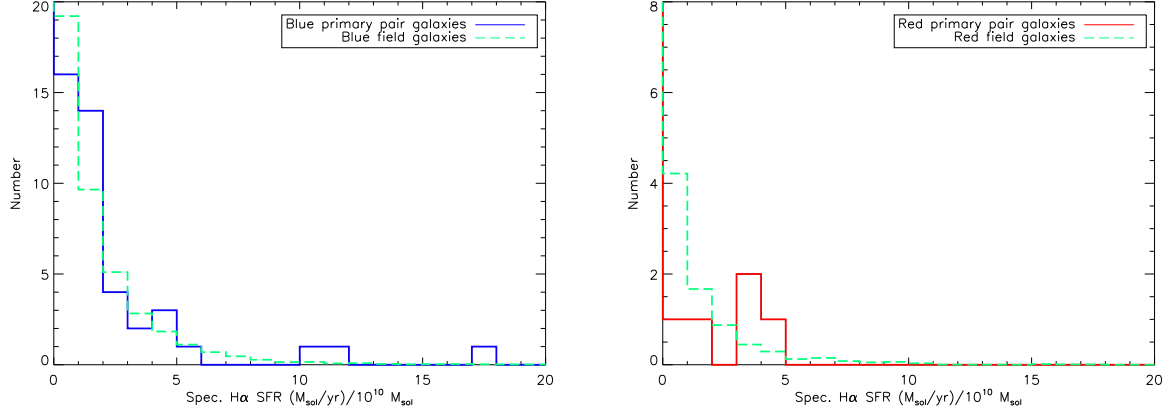


Fig. 14.— Distributions of SSFR for the blue primary galaxies (above left) and the red primary galaxies (above right) in the minor pairs sample, along with the average distribution of SSFR for the matched set of blue field galaxies.

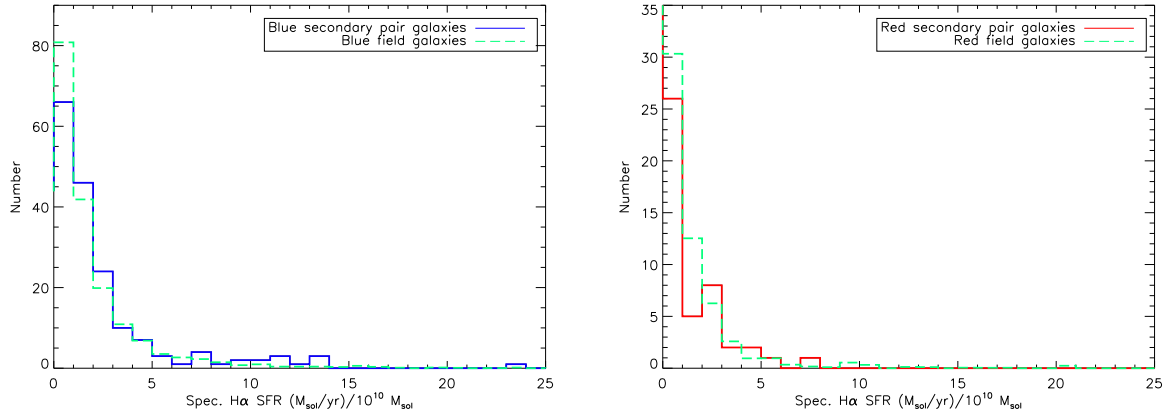


Fig. 15.— Distributions of SSFR for the blue secondary galaxies (above left) and the red secondary galaxies (above right) in the minor pairs sample, along with the average distribution of SSFR for the matched set of blue field galaxies.

Not all of the candidates for tidally triggered star formation actually exhibit enhanced star formation. Some of the apparent pairs may be superpositions and some of them may not yet have reached perigalacticon. Likewise, some of the galaxies with active star formation may not be reacting to the gravitational tidal interaction, but to supernova-enhanced star formation (Lada et al. 1978; Elmegreen et al. 1995; Boss 2003) for the less massive galaxies, or they may be interact-

ing with another companion hidden from our view on the far side of the galaxy. The galaxy morphology strongly influences the strength or duration of the tidally triggered star formation Mihos & Hernquist (1996); Tissera et al. (2002).

6. Specific Star Formation Rates and Pair Properties

Disparities in the SSFR distributions for major pair galaxies and the matched field samples suggest systematic differences in star formation properties of galaxies in pairs and in the field, but more conclusive evidence for tidally triggered star formation requires a measured dependence on a parameter of the interaction. We test the correlation between the specific star formation rate and the projected spatial separation of the galaxy pairs.

Barton et al. (2000) first showed that $\text{EW}(\text{H}\alpha)$ and ΔD are correlated for major pair galaxies in a sample drawn from the CfA2 Redshift Survey. A number of other studies have also shown a link between star formation rates and pair separation for major galaxy pairs (Lambas et al. 2003; Nikolic et al. 2004; Geller et al. 2006). Woods et al. (2006) examine the star formation properties of 57 galaxies in minor ($|\Delta m_r| > 2$) pairs, which do not show strong evidence for enhanced star formation rates. Here we examine a much larger sample that enables study of subsets of primary and secondary galaxies separately, and in subsets of color.

We find that the SSFR and ΔD are correlated in the secondary starforming galaxies in minor pairs, for both the blue and the red galaxy subsets. Table 2 gives a summary of the Spearman rank test correlation probabilities. Figure 16 shows the mean SSFR vs. ΔD for the minor interactions. The correlations between SSFR and ΔD in the minor secondary galaxies is detected even though the sample is deficient in close pairs. If our minor pairs sample had a flat distribution across ΔD , as it is should in a complete sample, we would expect to measure stronger correlations.

The primary starforming galaxies in minor pairs do not have a measurable correlation between SSFR and ΔD for either the blue or the red subsets. We note that it may be particularly difficult to observe triggered star formation in the minor primaries in our sample due to the deficiency in pairs at small ΔD . Our sample of minor primaries that are classified as blue starforming galaxies comprises 68 galaxies, and only 17 of those 68 galaxies have $\Delta D < 20 \text{ kpc h}^{-1}$. Even with a larger sample, we would expect the triggered star formation in the minor primaries to be weaker because galaxies with high luminosity tend to have lower gas contents. Additionally, simulations of the Milky Way and LMC interaction demonstrate an asymmetry in the response to the gravitational interaction of the primary and secondary galaxies in minor interactions, where the minor LMC is much more strongly affected than the Milky Way (Mayer et al. 2001; Mastropietro et al. 2005),

The previous studies of major galaxy interactions that have demonstrated a correlation between star formation indicators and projected separation are not segregated by color. Here, we test the contribution to the SSFR- ΔD correlation by the red and blue subsets of starforming galaxies. We find that the major galaxy pairs ($|\Delta m_z| < 2$) exhibit strong correlations between SSFR and ΔD

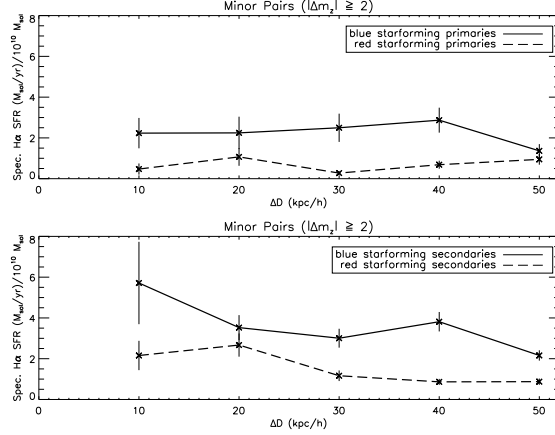


Fig. 16.— The mean SSFR per ΔD bin for the red and blue starforming galaxies in minor pairs. The Spearman rank test detects a correlation between the individual SSFR and ΔD for the blue and for the red secondary starforming galaxies, but not for the blue or for the red primary starforming galaxies.

for the blue galaxies (Table 2). This correlation holds for the blue primary and blue secondary galaxies in the major pairs when considered separately or together. The subsets of red starforming galaxies do not exhibit statistically significant correlations between SSFR and ΔD , although the plot of mean SSFR versus ΔD appears to suggest a trend in high SSFR at small ΔD (Figure 17). However, when we measure the correlation between SSFR and ΔD for the entire set of starforming galaxies in the major pairs sample, including both red and blue primaries and secondaries, we do detect a very strong correlation between SSFR and ΔD . Our results suggest that the blue starforming galaxies dominate the measurement of a correlation between formation indicators and projected separation in samples not separated by color.

The primary and secondary galaxies in major pairs exhibit symmetry in their response to the tidal interaction, in contrast to the minor pairs. Our results agree with those of Nikolic et al. (2004), who find that the relative z -band magnitude does not affect the star formation activity in their sample of SDSS pairs with $|\Delta m_z| < 2$. The CfA2 Survey galaxy pairs with $|\Delta m_R| < 2$ in the study by Woods et al. (2006) also show similar distributions of $EW(\alpha)$ across the range of small magnitude differences. Both the brighter and the fainter in the galaxy pairs with luminosity ratio $L_2/L_1 \leq 0.5$ ($|\Delta m| < 0.75$) show similar increases in stellar birthrates compared to field samples in the 2dF field galaxy pairs of Lambas et al. (2003); the galaxy pairs with $L_2/L_1 > 0.5$ show less star formation enhancement than pairs of similar luminosity. Our results are in general agreement with those of Lambas et al., except that we find the secondary galaxies in $|\Delta m_z| \geq 2$ pairs have more significantly enhanced SSFRs than the primaries; Lambas et al. find the opposite for in close ($\Delta D < 25$ kpc h^{-1}) pairs with $L_2/L_1 > 0.5$ ($|\Delta m| < 0.75$). It is unclear how the different distributions of relative magnitudes affect the comparison of our work with that of Lambas et al.

Table 2: Spearman rank tests of SSFR versus ΔD correlation for various samples.

Sample	P_{SR}	C_{SR}	Sample Size
Minor primary (blue SFG ^a)	0.46	-9.1×10^{-2}	68
Minor primary (red SFG)	0.68	6.6×10^{-2}	41
Minor secondary (blue SFG)	1.3×10^{-2}	-0.17	220
Minor secondary (red SFG)	9.3×10^{-3}	-0.24	118
Minor primary & secondary (blue & red SFG)	2.2×10^{-3}	-0.14	447
Major primary (blue SFG)	2.1×10^{-2}	-0.16	190
Major primary (red SFG)	0.53	-5.9×10^{-2}	118
Major secondary (blue SFG)	1.9×10^{-3}	-0.17	335
Major secondary (red SFG)	0.20	-0.10	167
Major primary & secondary (blue & red SFG)	4.1×10^{-4}	-0.12	810

^aSFG: Star Forming Galaxy.

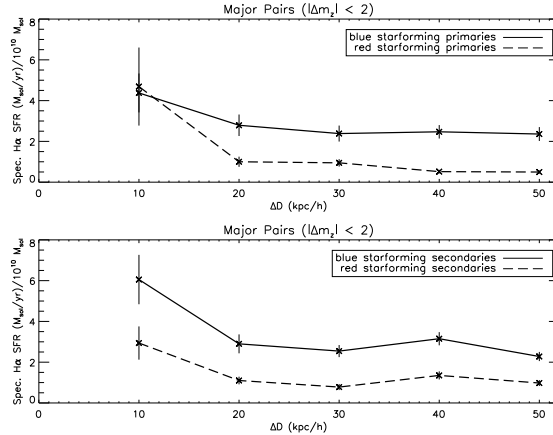


Fig. 17.— The SSFR per ΔD bin for the starforming galaxies in the major pairs samples. The Spearman rank test detects a correlation between the individual SSFR and ΔD for the blue primary starforming galaxies in the major pairs.

6.1. Concentration Index and Pair Properties

As a complement to studying the star formation rates, we also look for trends in the concentration index of the pair galaxies. The concentration index, C , defined here as the ratio of the radii of apertures containing 90% and 50% of the r -band Petrosian magnitude, can be linked to galaxy type and color (e.g. Strateva et al. 2001; Kauffmann et al. 2003a). Galaxies with concentration indexes in the range $2.0 < C < 2.6$ correspond to spiral and irregular types, while those with $C > 2.6$ usually correspond to early type galaxies (Strateva et al. 2001). A high value of C indicates a relatively bright central region. Nikolic et al. (2004) discuss the use of the concentration

index as a morphological indicator for interacting galaxies. They point out that late-type systems with strong central star formation would be wrongly categorized.

We avoid assigning a morphological type based on concentration index and instead examine the correlation between the concentration index and ΔD . The blue starforming secondary galaxies in the minor pairs exhibit a strong correlation between C and ΔD , the Spearman rank probability is $P_{SR} = 2.9 \times 10^{-5}$, where $C_{SR} = -0.28$. Hence, galaxies at small separations tend to have higher central concentrations of light. This result is consistent with the SSFR- ΔD correlation, suggesting that a central burst of star formation occurs in interacting galaxies, and is observed both in terms of a relatively bright central region and a high value of SSFR. Similarly, we do not measure a correlation between C and ΔD for the either the blue or red primary galaxies in the minor pairs. The concentration index- ΔD correlation for pair galaxies agrees well with the work of Nikolic et al. (2004), who measure a correlation between concentration index and ΔD in their sample of SDSS close pairs.

7. Specific Star Formation Rates and Galaxy Properties

In the previous section we compared the SSFRs for pair samples with matched sets of field galaxies and found systematic differences in their distributions in some cases. In this section we look more specifically at the SSFRs of pair galaxies as a function of M_z , compared to matched sets of field galaxies. Previous studies have yielded different conclusions on the role of intrinsic luminosity in affecting star formation activity in pair galaxies. Lambas et al. (2003) report no luminosity dependence for the mean star formation enhancement of their pair galaxies compared to representative field galaxies in their sample of close galaxy pairs ($\Delta D < 25 \text{ kpc h}^{-1}$ and $\Delta V < 100 \text{ km s}^{-1}$) in the 2dF Survey. However, they find that a higher fraction of the more luminous galaxies have a stellar birthrate parameter greater than the mean in their corresponding field sample.

Pair galaxies have a higher mean SSFR than field galaxies at every M_z in our combined sample of blue starforming galaxies in major and minor pairs (Figure 18). This result holds for our entire pairs sample with $\Delta D < 50 \text{ kpc h}^{-1}$, and for the subset of pairs with $\Delta D < 20 \text{ kpc h}^{-1}$, where the tidally triggered star formation should be strongest. We detect a very interesting trend in the mean SSFR as a function of M_z : pair galaxies with lower intrinsic luminosity have a greater relative increase in mean SSFR than pair galaxies with higher intrinsic luminosity, compared to matched sets of field galaxies (Figure 18). The relative increase in mean SSFR for the $\Delta D < 20 \text{ kpc h}^{-1}$ pair galaxies is more pronounced than for the $\Delta D < 50 \text{ kpc h}^{-1}$ pair galaxies, consistent with the idea that pairs at smaller ΔD being more strongly affected by the tidally triggered star formation. For the $\Delta D < 20 \text{ kpc h}^{-1}$ pairs, the slopes of the mean SSFR versus M_z for the pairs and for the field galaxies differ by almost 4σ . This general trend is insensitive to the binning of the M_z or the inclusion of the highest and lowest M_z bins.

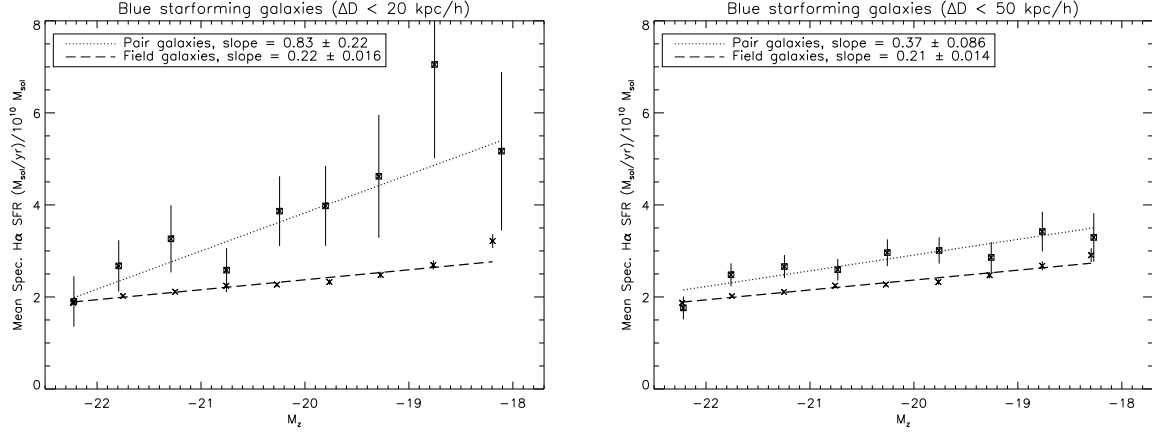


Fig. 18.— The mean SSFR as a function of M_z for the entire sample of blue starforming galaxies in major and minor pairs, and the mean SSFR for the matched sets of field galaxies. The plot on the left shows the pairs with $\Delta D < 20 \text{ kpc h}^{-1}$, and the plot on the right shows the pairs with $\Delta D < 50 \text{ kpc h}^{-1}$. Although the galaxies in pairs have greater mean SSFR at every M_z , the lower luminosity galaxies have greater enhancement in their mean SSFRs compared to the field sample.

Our large dynamic range in M_z ($-22.5 < M_z < -18$) contributes to our ability to detect the trend in increased SSFR as a function of M_z . Our sample includes such a large dynamic range because the galaxies in the minor pairs populate the extremes of the distribution (see the distributions of M_z in Figure 4). Lambas et al. may not have detected the trend in enhanced star formation as a function of luminosity because of their large uncertainty in the values of mean star formation excess compared to field galaxies (see Figure 8 in their paper).

The larger gas content that is expected in the lower luminosity pair galaxies compared to the more luminous pair galaxies probably contributes to their greater relative increase in SSFR over the matched sets of field galaxies. Measuring the gas content of the galaxies would help to determine its role in the greater relative increase in SSFR for lower luminosity galaxies. The relationship between relative increase in mean SSFR and M_z may also be attributed to pair properties such as $|\Delta m_z|$ (a proxy for the mass ratio); the galaxies at the extremes of the M_z range are mostly minor pairs. In §6 we show that the primary galaxies in minor pairs experience less triggered star formation than the secondary galaxies in minor pairs. A test of the influence of the relative magnitude on the relationship between increased SSFR and M_z requires a pairs sample that is large enough to measure mean SSFR for pairs compared to field galaxies for galaxy pairs segregated by $|\Delta m_z|$ across a wide range in M_z .

8. Conclusions

We study a sample of 1204 galaxies in minor pairs ($|\Delta m_z| \geq 2$) and 2409 galaxies in major pairs ($|\Delta m_z| < 2$) drawn from the SDSS DR5. We classify the galaxies in our pairs sample as starforming galaxies, composites, or AGNs, and separate by color to distinguish intrinsic galaxy properties from properties of the interaction. Our results suggest that gravitational tidal interactions trigger bursts of star formation in cases where the gravitational tidal force is relatively strong compared to the self-gravity of the galaxy: the secondary galaxy in minor pairs is more strongly affected by the interaction than the primary galaxy; both galaxies in major interactions show enhanced star formation. Blue galaxies appear to be more susceptible to tidally triggered star formation than red galaxies, probably resulting from their higher gas content (Barnes & Hernquist 1996).

In the sample of minor pairs, the secondary galaxies show a correlation between SSFR and ΔD , for both subsets of blue and red starforming galaxies. The primary galaxies in the minor pairs sample do not have measurable correlations between SSFR and ΔD ; however, this subset may be particularly disadvantaged by the lack of pairs at small separation. Measurement of the correlation between the concentration index C and ΔD for our minor pair galaxies supports our SSFR - ΔD results: the blue secondary galaxies show a correlation between high values of C and small ΔD ; the red secondary galaxies do not. Large C corresponds to centrally bright galaxies, which may be experiencing a burst of central star formation.

For the galaxies in major interactions, the subsets of blue starforming primaries and blue starforming secondaries both show a correlation between the SSFR and ΔD , while the subsets of red starforming galaxies do not. A consistent explanation for these observations is that the blue galaxies tend to be more gas-rich than the red galaxies. When the galaxy experiences a gravitational tidal force from its companion, the gas is driven to the center, where a burst of star formation occurs. The red galaxies, which tend to be gas-poor, have little material available to form new stars, even if they experience gravitational tidal forces (Barnes & Hernquist 1996). Comparison of the distribution of SSFRs of the major pair galaxies with matched subsets of field galaxies reveal statistical differences for the blue galaxies, again suggesting that the blue galaxies in major pairs experience enhanced star formation rates.

Galaxies in pairs have higher mean SSFR at every absolute magnitude compared to matched sets of field galaxies. The relative increase in SSFR depends on the intrinsic luminosity of the galaxy; galaxies with lower intrinsic luminosities show a greater relative increase in mean SSFR compared to matched sets of field galaxies than galaxies with high intrinsic luminosities do. Our pairs sample is the first to show this trend conclusively because of the large dynamic range in M_z ($-22.5 < M_z < -18$). Including both major and minor encounters allows us to obtain the large dynamic range because the extremes of the range are populated mainly with minor pairs.

The greater relative increase in SSFR compared to the matched sets of field galaxies for the lower luminosity galaxies may be attributable to their larger gas content compared to high luminosity galaxies, or it may be attributable to pair properties such as $|\Delta m_z|$. Measuring the gas

content of the galaxies is important for determining its role in the greater relative increase in SSFR for lower luminosity galaxies. It would also be useful to obtain a pairs sample that is large enough to separate into $|\Delta m_z|$ subsets across a wide range in M_z .

Our sample hints at triggered AGN activity in pair galaxies. The fraction of AGN is greater in the pairs samples compared to matched sets of field galaxies with similar distributions of absolute magnitude and color. We also find that the fraction of objects classified as AGN increases at small ΔD for the primary galaxies in minor interactions. The triggered AGN observations are enticing but not conclusive: small aperture spectroscopy for pairs at small apparent separations are needed.

A consistent picture on the effects of tidal triggering is emerging in a variety of pairs samples. Clarification of the outstanding issues requires better sampling at small ΔD for a large dynamic range of intrinsic luminosities, and measurements of the gas content of the galaxies. Comparisons with model predictions of observable parameters would also contribute to a detailed understanding of tidally triggered star formation and AGN activity.

9. Acknowledgments

The authors thank Elizabeth Barton, Lisa Kewley, and Daniel Fabricant for discussions that helped to improve this paper. We thank Bill Wyatt for maintaining a local copy of the SDSS data products at the Harvard-Smithsonian Center for Astrophysics.

Our research has made use of NASA's Astrophysics Data System Bibliographic Services. This work is funded in part by the Smithsonian Institution.

Funding for the SDSS and SDSS-II has been provided by the Alfred P. Sloan Foundation, the Participating Institutions, the National Science Foundation, the U.S. Department of Energy, the National Aeronautics and Space Administration, the Japanese Monbukagakusho, the Max Planck Society, and the Higher Education Funding Council for England. The SDSS Web Site is <http://www.sdss.org/>.

The SDSS is managed by the Astrophysical Research Consortium for the Participating Institutions. The Participating Institutions are the American Museum of Natural History, Astrophysical Institute Potsdam, University of Basel, University of Cambridge, Case Western Reserve University, University of Chicago, Drexel University, Fermilab, the Institute for Advanced Study, the Japan Participation Group, Johns Hopkins University, the Joint Institute for Nuclear Astrophysics, the Kavli Institute for Particle Astrophysics and Cosmology, the Korean Scientist Group, the Chinese Academy of Sciences (LAMOST), Los Alamos National Laboratory, the Max-Planck-Institute for Astronomy (MPIA), the Max-Planck-Institute for Astrophysics (MPA), New Mexico State University, Ohio State University, University of Pittsburgh, University of Portsmouth, Princeton University, the United States Naval Observatory, and the University of Washington.

REFERENCES

Adelman-McCarthy, J., Agueros, M.A., Allam, S.S., et al. 2006, ApJS, 162, 38

Alonso, M. S., Lambas D. G., Tissera, P., & Coldwell, G. 2007, MNRAS, ...

Arp, H. 1966, Atlast of Peculiar Galaxies. California Inst. of Technology, Pasadena

Ball, N. M., Loveday, J., Brunner, R. J., Baldry, I. K., Brinkmann, J. 2006, MNRAS, 373, 845

Barnes J. E. & Hernquist L. E., 1991, ApJ, 370, L65

Barnes J. E. & Hernquist L., 1996, ApJ, 471, 115

Barton Gillespie, E., Geller, M. J. & Kenyon, S.J. 2003, ApJ, 582, 668

Barton, E. J., Geller, M.J., & Kenyon, S.J. 2000, ApJ, 530, 660 (BGK)

Baldry I. K., Glazebrook K., Brinkmann J., Ivezic, Ž., Lupton R. H., Nichol R. C., Szalay A. S., 2004, ApJ, 600, 681

Bernardi, M. et al. 2003, AJ, 125, 1882

Best, P. N., Kauffmann, G., Heckman, T. M., Brinchmann, J., Charlot, S., Ivezic, Ž., & White, S. D. M. 2005, MNRAS, 362, 25

Boss, A. P. 2003, in ASP Conf. Ser. 287, Galactic Star Formation Across the Stellar Mass Spectrum, ed. J. M. De Buizer & N. S. van der Blieck (San Francisco: ASP), 281

Bushouse, Howard A. 1987, ApJ, 320, 49

Carter, B. J., Fabricant, D. G., Geller, M. J., Kurtz, M. J., & McLean, B. 2001, ApJ, 559, 606

Conselice, Christopher, J. 2006, MNRAS, 373, 1389

Cox, T. J., Jonsson, P., Primack, J. R., Somerville, R. S. 2006, MNRAS, 373, 1013

Dahari, O. 1985, ApJS, 57, 643

Diaferio, A., Kauffmann, G., Colberg, J. M., & White, S. D. M. 1999, MNRAS, 307, 537

Donzelli, C. J. & Pastoriza M. G. 1997, ApJS, 111, 181

Dressler, A. 1980, ApJ, 236, 351

Elmegreen, B. G., Kimura, T., & Tosa, M. 1995, ApJ, 451, 675

Freedman Woods, D., Geller, M. J., & Barton, E. B. 2006, AJ, 132, 197

Fuentes-Williams T.& Stocke J. T., 1988, AJ, 96, 1235

Fukugita, M., Ichikawa, T., Gunn, J.E., Doi, M., Shimasaku, K., & Schneider, D.P. 1996, AJ, 111, 1748

Geller, Margaret J., Kenyon, Scott J., Barton, Elizabeth J., Jarrett, Thomas H., Kewley, Lisa J. 2006, AJ, 132, 2243

Gómez, P. L. et al. 2003, ApJ, 584, 210

Gunn, J.E., Siegmund, W.A., Mannery, E.J., Owen, R.E., et al. 2006, AJ, 131, in press (astro-ph/0602326)

Gunn, J.E., Carr, M.A., Rockosi, C.M., Sekiguchi, M., et al. 1998, AJ, 116, 3040

Hashimoto, Y., Oemler, A. J. Lin, H., & Tucker, D. L. 1998, ApJ, 499, 589

Hennawi, J. F., et al. 2006, AJ, 131, 1

Hernquist L., 1989, Nat, 340, 687

Hernquist, L. & Mihos, J. C. 1995, ApJ, 448, 41

Hopkins, A. M., Miller, C. J., Nichol, R. C., Connolly, A. J., Bernardi, M., Gómez, P. L., Goto, T., Tremonti, C. A., Brinkmann, J., Ivezić, Ž., Lamb, D. Q. 2003, ApJ, 599, 971

Hopkins, P. F., et al. 2006, ApJS, 163, 1

Hummel, E. 1981, A&A, 96, 111

Jansen, R. A., Franx, M., Fabricant, D., & Caldwell, N. 2000a, ApJS, 126, 271

Jansen, R. A., Knapen, J. H., Beckman, J. E., Peletier, R. F., & Hes, R. 1994, MNRAS, 270, 373

Jarrett, T. H., Chester, T., Cutri, R., Schneider, S., Skrutskie, M., & Huchra, J. P. 2000, AJ, 119, 2498

Jones, B. & Stein, W. A. 1989, AJ, 98, 1557

Kauffmann, G., Colberg, J. M., Diaferio, A. & White, S. D. M. 1999a, MNRAS, 303, 188
— 1999b, MNRAS, 307, 529

Kauffmann, G., et al. 2003a, MNRAS, 341, 54

Kauffmann G. et al., 2003b, MNRAS, 346, 1055

Kauffmann, G., White, S. G., Heckman, T. M., Ménard, B., Brinchmann, J., Charlot, S. Tremonti, C., Brinkmann, J. 2004, MNRAS, 353, 713

Kauffmann, G., & Haehnelt, M. 2000, MNRAS, 311, 576

Keel, W. C. 1993, AJ, 106, 1771

Keel, W. C., Kennicut, R. C. Jr, Hummel, E., & van der Hulst, J. M. 1985, AJ, 90, 708

Kelm, B., Focardi, P., & Zitelli, V. 2004, A&A, 418, 25

Kennicutt, R. C., Jr. 1998, ARA&A, 36, 189

Kennicutt, R. C. & Keel, W. C. 1984, APJ, 279, L5

Kennicutt, R. C., Jr., Keel, W. C., van der Hulst, J. M., Hummel, E., & Roettiger, K. A. 1987, AJ 95, 5

Kewley, Lisa J., Jansen, Rolf A., Geller, Margaret J. 2005, PASP, 117, 227

Kewley, L., Groves, B., Kauffmann, G., Heckman, T. 2006, MNRAS, 372, 961

Lada, C. J., Elmegreen, B. G., & Blitz, L. 1978, in Protostars and Planets: Studies of Star Formation and of the Origin of the Solar System, ed. T. Gehrels (Tucson: Univ. Arizona Press), 341

Lambas, D. G., Tissera, P. B., Alonso, M. S., & Coldwell, G. 2003, MNRAS, 346, 1189

Larson, R. B. & Tinsley, B. M. 1978, ApJ, 219, 46

Lewis, I. et. al. 2002, MNRAS, 334, 673

Liu, C. T. & Kennicutt, R. C., Jr. 1995, ApJ, 450, 547

Mastropietro, C., Moore, B., Mayer, L. Wadsley, J. & Stadel, J. 2005, MNRAS, 363, 509

Mayer, L. Governato, F., Colpi, M., Moore, B., Quinn, T. R., Baugh, C. M. 2001, Ap&SS, 276, 375

Mihos, J. C. & Hernquist, L. 1996, ApJ, 464, 641

Negroponte J., White S. D. M., 1983, MNRAS, 205, 1009

Nikolic, B., Cullen, H. & Alexander, P. 2004, MNRAS, 355, 874

Padmanabhan, N., White, M., & Eisenstein, D. 2006, astro-ph/0612013

Petrosian, V. 1976, ApJ, 209, L1

Rines, K., Geller, M. J., Kurtz, M. J., & Diaferio, A. 2005, AJ, 130, 1482

Sandage, A. & Visvanathan, N. 1978, ApJ, 223, 707

Schmitt H. R., 2001, AJ, 122, 2243

Serber, W., Bahcall, N., Méndard, B., & Richards, G. 2006, ApJ, 643, 68

Sekiguchi, K. & Wolstencroft, R. D. 1992, 255, 581

Somerville, R. S. & Primack, J. R. 1999, MNRAS, 255, 581

Spergel, D. N., et al. 2003, ApJS, 148, 175

Strateva, I. et al. 2001, AJ, 122, 1861

Strauss, M.A., Weinberg, D.H., Lupton, R.H. et al. 2002, AJ, 124, 1810

Struck, C. 2005, Astrophysics Update Vol. 2, in press

Tissera P. B., Domnguez-Tenreiro R., Scannapieco C., & Sàiz A. 2002, MNRAS, 333, 327

Toomre A. & Toomre J., 1972, AJ, 178, 623

Wechsler, R. H., Bullock, J. S., Primack, J. R., Kravtsov, A. V., Dekel, A. 2002, ApJ, 568, 52

Yasuda, N. et al. 2001, AJ, 122, 1104

York, D.G., Adelman, J., Anderson, J.E., et al. 2000, AJ, 120, 1579